DEVELOPMENT OF A CRYOCATCHER-SYSTEM FOR SIS100*

L. Bozyk[1,2], P. Spiller[2], H. Kollmus[2]
[1]TU-Darmstadt, Germany; [2]GSI Darmstadt, Germany

Abstract

The main accelerator SIS100 of the FAIR-facility will provide heavy ion beams of highest intensities using intermediate charge state heavy ions. Ionization beam loss is the most important loss mechanism, therefore, a special synchrotron layout has been developed, which includes a dedicated cold ion catcher system which provides almost hundred percent catching efficiency. Dynamic vacuum effects are suppressed effectively by means of special low desorbing surfaces. A prototype of the cryocatcher has been developed, constructed and tested with heavy ion beams from SIS18. It is a workpackage of the EU-FP-7 project COLMAT. Results from these tests are presented, as well as implications for the production of the 60 SIS100 cryocatchers.

ION CATCHER SYSTEM FOR SIS100

For heavy ion operation the reference projectile is U^{28+}. The ion optical lattice of SIS100 has been optimized such that stripped beam ions (U^{29+}) are lost at well defined highly localized positions in the cryogenic arcs [1]. This allows the installation of an efficient ion catcher system with perpendicular low desorption surfaces. Thereby, the amount of charge exchange processes in collisions with residual gas molecules and consecutive ionization beam loss is stabilized during operation.

Basic design considerations of the cryocatcher system were presented in [2]. A prototype has been designed, constructed, build, and tested with liquid helium and heavy ion beams from SIS18. This test setup and first results were presented in [3]. Results have been evaluated carefully and implications on the SIS100 cryocatcher are presented. A complete overview about the cryocatcher can be found in [4].

PROTOTYPE CRYOCATCHER

The cryocatcher consist of a gold coated low desorbing copper block inside a vacuum chamber, plated with copper from outside. The copper ensures a homogeneous low temperature distribution at cryogenic temperatures in order to provide a high pumping surface. A special support structure allows to keep the cryocatcher at a higher temperature than the chamber. This avoids the adsorption of resiudal gas on the surface of ion impact, to keep the desorption low. The cryocatcher prototype is mounted inside a dedicated cryostat. A sketch of the whole test-setup is shown in figure 1. It contains several vacuum-, beam-, and temperature-diagnostics. Via a cold-warm-transition the cold chamber is connected to a room temperature beam line in the experimental cave HHT at GSI. It is equipped with vacuum- and beam-diagnostics as well as vacuum infrastructure. The cryocatcher was irradiated directly with heavy ion beams and the ion impact induced pressure rise inside the chamber was measured. For pressure measurements an extractor gauge with hot filament is placed next to the cryocatcher. The thermal radiation is screened and the heat load of the hot filament is dissipated into the thermal shield which is cooled with liquid nitrogen. A fast and beam impact triggered pressure readout was realized, to measure the pressure rises due to ion impact and the pressure decay due to cryosorption.

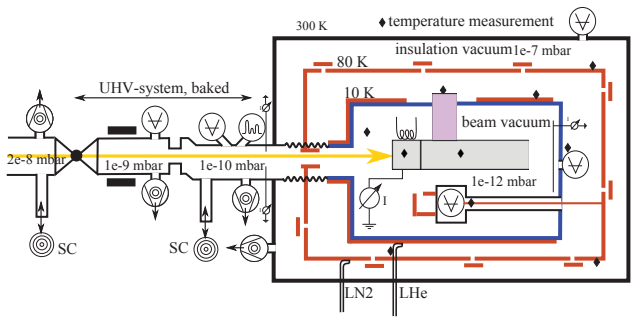

Figure 1: Sketch of the cryocatcher prototype test setup: The cryocatcher is located inside a liquid helium cooled vacuum chamber, mounted inside a dedicated cryostat. Via a cold-warm-transition the cold chamber is connected to warm diagnostics, vacuum infrastructure, and a GSI-beamline for heavy ion beams.

The temperature measurements were used to verify temperature models, measure heat loads, have reference temperatures for pressure measurements, and to control the cooling. The position of the beam was adjusted with two scintillating targets in the warm sections and controlled by the electrically insulated front part of the cryocatcher and several insulated plates in the cryogenic environment. Two different cryocatcher geometries were tested: A block catcher, similar to the established geometries in SIS18 and a stair-like catcher, which provides perpendicular incidence and shielding of desorbed molecules from the beam axis.

RESULTS FROM MEASUREMENTS

During the cold tests temperatures down to 10 K at the cold chamber and residual gas pressures in the low

* Work supported by EU (FP7 workpackage COLMAT) and GP-HIR – Graduate Program for Hadron and Ion Research at GSI

ISBN 978-3-95450-115-1

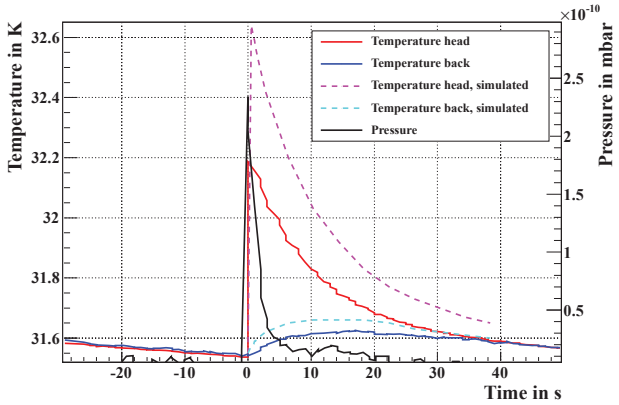

Figure 2: Pressure and temperature evolution at the cryocatcher. The thermal reaction can be reproduced with ANSYS-simulations.

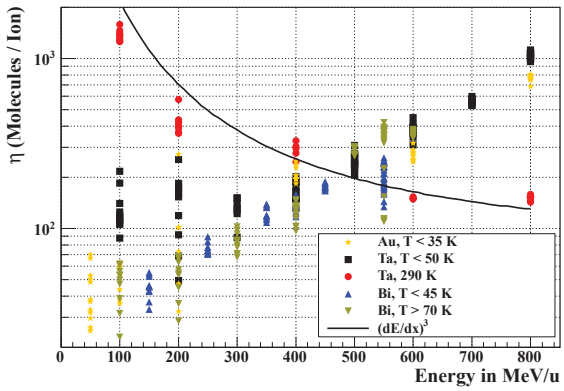

Figure 3: Desorption yields which were measured at the cryocatcher during different beamtimes.

10^{-12} mbar-regime could be reached. Beam impacts could be observed in the temperature measurements at the cryocatcher, the residual gas pressure evolution, and the electrical current on the cryocatcher's head.

Figure 2 shows temperature and pressure evolution during the impact of $1.12 \cdot 10^9$ 800 MeV/u Ta-ions onto the cryocatcher. Both, temperature of the cryocatcher and the pressure show a fast, beam induced rise, followed by a slow decay. The temperature of the backside follows due to thermal conductance and capacity with a damped delay. Also the temperature of the support responds to beam impacts. The thermal reaction of the cryocatcher can be reproduced with ANSYS simulations. In the simulations the temperature directly on the surface of the cryocatcher was calculated, the small difference less than 400 mK between measured and simulated evolution is due to the neglected thermal capacity and conductance of the temperature sensors. So it is possible to verify the thermal stability of the cryocatcher for different loss scenarios in SIS100.

The temperature of the cryocatcher could be varied by 40 K while the temperature of the vacuum chamber only changed by less than 2 K. The support of the cryocatcher provides a high thermal resistance and thus fulfills its requirements.

The difference between peak and relaxation pressure gives the ion induced pressure rise Δp. Using the number of incident particles N_{Ion}, the gas temperature which is equivalent to the chamber temperature T, and the chamber volume V, a desorption yield η is calculated:

$$\eta = \frac{\Delta p}{N_{\mathrm{Ion}}} \cdot \frac{V}{k_B \cdot T}$$

During beamtimes with Gold, Tantalum, and Bismuth, η was investigated as a function of ion energy and cryocatcher temperature. The measured yields are shown in figure 3. From room temperature measurements a scaling of the desorption yield with the electronic energy to the second to third power is known [5, 6]. This behavior could be reproduced at room temperature, whereas at cryogenic temperatures a contrary scaling was observed. In the investigated energy and temperature interval (30 K - 90 K) this scaling shows no dependence on the temperature of the cryocatcher. Crossing the vapor pressure curve of CO_2 around 63 K without any reaction of η shows, thtat no cryocondensation, but only cryoadsorption at higher temperatures takes place on the cryocatcher. During the Bismuth beamtime the stair-like cryocatcher was used, but no significant screening of desorbed gases could be observed.

During cooldowns and warmups the transition temperature of ∼18 K, underneath a pumping speed for hydrogen emerges, could be verified several times. Each time lowering the chamber temperature below the transition temperature, the pressure dropped by two orders of magnitude within several minutes. Excessing the temperature results in a fast pressure rise by several orders of magnitude, as all adsorbed gases on the surface get released quickly.

The slow pressure decay after beam impacts was used to estimate pumping speeds. A qualitative saturation of the cold surfaces could be observed. Shortly after falling below the transition temperature, the highest pumping speed could be measured. This pumping speed decreases with time, as gases from the warm sections flow into the cold chamber, saturating the surfaces. Having fully saturated surfaces the pumping speed adopts the same value as if the temperature is above 20 K. Dedicated measurements will investigate the hydrogen pumping and its saturation.

The measured electrical current on the cryocatcher head was used to calculate the secondary electron yields in figure 4. It scales with the electronic energy loss as expected from [7]. But the magnitude is reduced by a factor 5, which can be explained by a reduced electron mobility in a cryogenic target compared to room temperature measurements in [7].

The measured desorption yields are described by a parabola to be used in dynamic vacuum simulations of SIS100 with StrahlSim [8]. The increasing yields are compensated by decreasing charge exchange cross section dur-

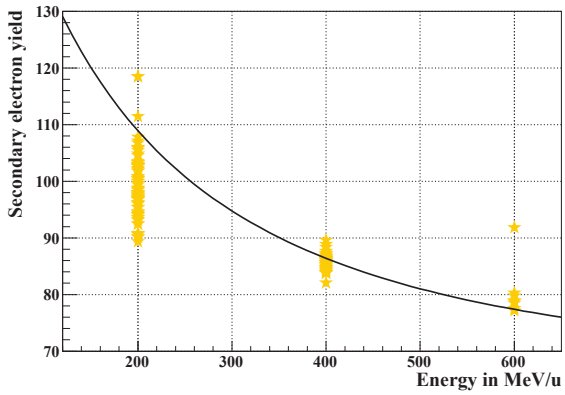

Figure 4: Secondary electron yield measured at the cryocatcher during Gold-beamtime compared to the electronic energy loss in arbitrary units.

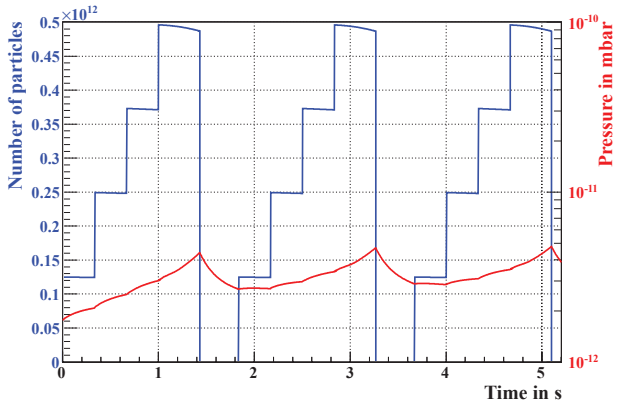

Figure 5: Simulated intensity and average residual gas pressure development during SIS100 cycles, using the measured desorption yields.

ing acceleration. This results in a stable cycle with intensities of $5 \cdot 10^{11}$ U^{28+} particles, see figure 5.

IMPLICATIONS FOR THE SIS100 CRYOCATCHER SYSTEM

Since the tests and measurements of the prototype were successful, the SIS100 series cryocatcher can be specified and constructed on the basis of the prototype. Nevertheless, the measurements give some implications for the SIS100 cryocatcher. It is important to stay below the transition temperature, to have a reliable pumping speed. The gas flow into the cold sections has to kept low, to preserve the pumping speed. The room temperature parts of the pumping posts therefore should be equipped with additional hydrogen pumps, e.g. NEG cartriges. Since beam impacts were visible at the temperature measurements in the insulating vacuum on the support of the cryocatcher, a temperature sensor not necessarily has to be mounted on the cryocatcher itself in the beam vacuum. The temperature of the cryocatcher could be adjusted by a heater element on the support, in order to assure the cryocatcher remains warmer than its surrounding during cooldown. This is necessary to keep the initial surface adsobates low.

The temperature of the thermal shield in SIS100, where the cryocatcher will be thermally connected to, is planed to vary between 50 K and 80 K along one arc. As in the investigated temperature interval the desorption yield is independent of the temperature of the cryocatcher, this represents no issue. Regardless, this connection has to remove the deposited energy from lost ions [9] reliable. Thermal simulations of the cryocatcher verified the thermal stability of the cryocatcher for high loss scenarios.

These thermal simulations hint, that by choosing a different material for the head of the cryocatcher, the desorption yield could be optimized. By changing the temperature of the cryocatcher from room temperature to cryogenic temperatures, its thermal capacity drops, while its conductivity rises. Such, the energy from beam ions, which gets absorbed deep inside the material, propagates more efficient to the surfaces, where desorption is triggered. Dedicated measurements on cryogenic desorption will show, if an optimized material can be found.

According to this consideration, the screening effect of the stair-like cryocatcher is compensated by its bigger surface. A calibration of the electrical current measurement is complicated, because no visible dependence of the beam energy could be observed. Additionally the manufacturing is more complicated for which reason the block geometry is preferred.

The length of the head of the cryocatcher is chosen such that lost beam ions get completely stopped inside. This divides the cryocatcher into a high and a low activated part. After the measurements only few activation of the backside could be measured. The activation of the front part mainly consists of Cobalt isotopes, with a maximum half life of 5.2 years.

CONCLUSION

The cryocatcher fulfills its requirements and makes sure, no vacuum instabilities and self amplifying ionization losses occur in SIS100.

REFERENCES

[1] P. Spiller et al., Proc. of ICFA04 (2005)

[2] L. Bozyk et al., Proceedings of IPAC'10 (2010)

[3] L. Bozyk et al., Proceedings of IPAC'11 (2011)

[4] L. Bozyk, Dissertation TU-Darmstadt, Germany (2012)

[5] H. Kollmus et al., J. Vac. Sci. Technol. A 27, 245 (2009)

[6] A. W. Molvik et al., Phys. Rev. Lett. 98, 064801 (2007)

[7] H. Rothard et al., Phys. Rev. A 41, 2521 (1999)

[8] P. Puppel, Dissertation, Goethe-Universität Frankfurt, Germany (2012)

[9] P. Puppel et al., Proceedings of IPAC'11 (2011)

ISBN 978-3-95450-115-1